ELSEVIER

Journal of Power Sources 95 (2001) 79–84

JOURNAL OF POWER SOURCES

www.elsevier.com/locate/jpowsour

Progressive changes in positive active material over the lifetime of a lead–acid battery

Ian M. Steele[a,*], Joseph J. Pluth[a], James W. Richardson Jr.[b]

[a]*Department of the Geophysical Sciences, The University of Chicago, Chicago, IL 60637, USA*
[b]*Argonne National Laboratory, Argonne, IL 60439, USA*

Abstract

Time-of-flight neutron diffraction for a series of lead–acid battery positive plate samples has shown that β-PbO_2 is not stoichiometric, but has a deficiency of Pb relative to oxygen giving $Pb_{0.92}O_2$ to $Pb_{0.96}O_2$. The Pb vacancies cause a charge deficiency that is balanced by crystallographic hydrogen on a disordered site. The position of hydrogen is typical of hydrogen bonding as has been previously proposed based on nuclear magnetic resonance spectra. With either rapid or conventional charging, the amount of hydrogen substitution decreases and the β-PbO_2 tends toward a stoichiometric composition at battery failure. High resolution SEM imaging of these and other battery samples shows a progressive change in the morphology of β-PbO_2 and these changes appear to be the same for both rapid or conventional charging. The morphology progresses from elongated, well-formed crystals to equidimensional crystals to dense clusters of crystals with a consequent reduction in surface area. Neither stoichiometry nor morphology changes necessarily contribute to battery failure, but both progressively change over the cycle life of the battery. © 2001 Elsevier Science B.V. All rights reserved.

Keywords: β-PbO_2; Rapid charging; Morphology; Hydrogen; Stoichiometry

1. Introduction

Lead–acid batteries undergo various changes over their useful life with some or all of these changes contributing to capacity loss. Many of these changes have been well documented and include, for example, grid corrosion and shedding of active material, both of which can be easily recognized. Other changes are less easy to recognize, but are well documented and might include sulfation, changes in conductivity of the active material, movement and concentration of contaminant or added minor or trace elements, and a decrease in catalytic recombination in valve regulated batteries. These and other changes can be recognized rather easily by routine laboratory examination or testing. The changes to be described here are those which have been observed in the positive active material using techniques not generally available and are probably impossible to recognize by casual examination or even routine laboratory instrumentation. These observations include crystallographic details of the β-PbO_2 crystal structure and modification of the morphology of individual β-PbO_2 crystals over the life of a lead–acid battery. We emphasize that the progressive changes we describe here are not proven to cause capacity loss and eventual failure, but do represent possible contributions which affect the characteristics of the positive active material.

2. Experimental

Two series of samples were available from Cominco Ltd., which resulted from their ALABC (Advanced Lead Acid Battery Consortium) studies. Details including the history and physical description for each sample are given in their final reports RMC-002 and RMC-002A to ALABC [1]. The first series of four samples represents a sequence from initial formation (five cycles) to battery failure (253 cycles) where conventional charging was used. The second series of five samples represents a sequence which underwent rapid charging with a range from 73 to 1056 (battery failure) cycles. A summary of these samples with cross references to Cominco designations is given in Table 1. Individual samples were represented by ~1 $in.^2$ sections of each plate, 1/16 in. thick. Each sample was in the charged state with minimal $PbSO_4$ such that the dominant material was β-PbO_2 and Pb metal from the grid. These nine samples were used for both neutron diffraction and for SEM studies.

In addition to the above samples, a sequence of 12 samples was obtained using a laboratory supplied charging

* Corresponding author. Tel.: +1-773-702-8109; fax: +1-773-702-9505.
E-mail address: steele@geosci.uchicago.edu (I.M. Steele).

0378-7753/01/$ – see front matter © 2001 Elsevier Science B.V. All rights reserved.
PII: S0378-7753(00)00610-8

Table 1
Charging conditions and number of cycles for Cominco supplied samples

Cominco designation	Number of cycles	
	Conventional	Rapid
Optima U	5	
Optima X	51	
Optima V	102	
Optima S	253	
Optima I		73
Optima Z		128
Optima R		243
Optima P		909
Optima W		1056

station courtesy of GNB Technologies. Using pasted and cured positive and negative plates supplied by GNB, a flooded cell was constructed and cycled to physical failure using a rapid charging algorithm programmed by GNB. After each 10 cycles a small amount of positive active material was sampled in the charged state for SEM study.

2.1. Neutron diffraction

Details of the diffraction experiment and data analysis will be presented elsewhere. For present purposes, time-of-flight diffraction spectra were obtained for nine samples using the Intense Pulsed Neutron Source at the Argonne National Laboratory, USA. Data collection time ranged from 15 to 24 h. Data reduction using standard Rietveld techniques resulted in cystallographic details for β-PbO_2 in each sample including lattice parameters, positional parameters for O, thermal parameters for both Pb and O, and occupancy fraction of Pb relative to oxygen. These data are summarized in [2]. While Rietveld analysis allows many choices in the data processing procedure such as algorithms for background and peak fitting, the results were essentially independent of these choices and convergence of the least squares refinement and parameter values were essentially the same.

2.2. Diffraction results

Two aspects of the β-PbO_2 crystal structure showed progressive changes over the battery life both for rapid and conventional charging. These two changes involved the shape of the displacement ellipsoid for Pb and the ratio of Pb to O, or the deviation from stoichiometry of β-PbO_2. The changes of the displacement ellipsoid have previously been described [2], while here we concentrate on the stoichiometry that has other implications. Non-stoichiometry of β-PbO_2 has long been recognized (e.g. [3]), but its characterization is based on either bulk chemical analyses or X-ray data for β-PbO_2. The present measurements are based on neutron interactions for which Pb and O have similar influence on the data in contrast to X-ray measurements where Pb dominates data.

It is important to recognize that diffraction results will only apply to crystallographic sited species. Thus, either Pb or O located at interstitial sites, particle boundaries, or otherwise non-crystallographic sites will not be sampled. Our results provide: (1) a ratio of Pb to O and (2) cannot allow for an atom population greater than allowed by the crystallographic site. For reason (2), we assume full occupancy of the more abundant species, for β-PbO_2, this is O, and Pb is thus less than full occupancy. Fig. 1a and b show the resulting occupancy of Pb as a function of cycle life for both rapid and conventional charging. For Fig. 1a, cycle life is expressed as the number of cycles, while in Fig. 1b cycle life is expressed as a percent of total life.

These occupancy data show: (1) that the β-PbO_2 structure is not stoichiometric and has a deficiency of Pb relative to O; (2) initially the stoichiometry can be expressed as ~$Pb_{0.92}O_2$ and becomes more stoichiometric in an approximately linear trend to reach $Pb_{0.96}O_2$ at about 250 cycles; (3) stoichiometry changes appear to be very similar regardless of the type of charging; (4) for rapid charging, the stoichiometry remains near $Pb_{0.96}O_2$ over a long cycling interval till failure; (5) for charge neutrality, another element must be present either on a lattice site or interstially, but in either case compensating for the deficiency of Pb positive charge.

2.3. Discussion of diffraction results

There have been many reports of evidence for the association of hydrogen with the β-PbO_2 structure, e.g. [4].

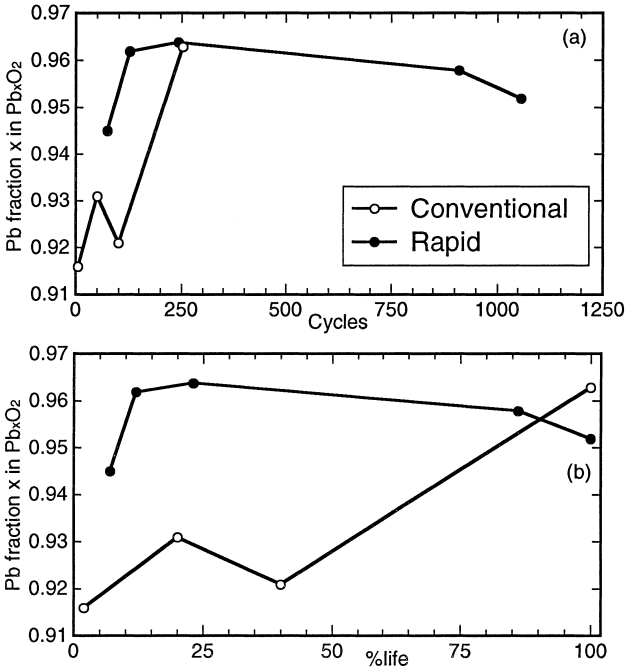

Fig. 1. Pb atomic fraction x in β-Pb_xO_2 based on neutron diffraction. Samples obtained from Cominco projects: (a) variation of x with cycles of either rapid or conventional charging; (b) variation of x expressed as percent of battery life.

In short, it is generally agreed that initial electro-formed β-PbO_2 has a relatively high concentration of H which upon cycling decreases with the β-PbO_2 tending to stoichiometry [5], although evidence to the contrary has been given [13]. It is not certain how the H is associated, but suggested possibilities include: (1) structural hydrogen; (2) OH or H_2O trapped at interface boundaries; (3) adsorbed water and (4) trapped water droplets. This H loss trend is consistent with the stoichiometry changes outlined above based on neutron diffraction results suggesting that in part the decrease in bulk hydrogen can be associated with the loss of structural hydrogen. Using difference Fourier techniques, we examined the nine data sets searching for indications of the presence of hydrogen on a crystallographic site. On each difference map, there was a negative peak at approximately the same location. While the magnitude of the peak was greatest for sample C5, the magnitudes of this negative peak for the remaining eight samples did not form a consistent trend possibly due to errors associated with the small peak. The significance of a negative peak is that hydrogen has a negative scattering intensity for neutrons. The position of this peak is not well defined and all attempts to refine position and extract the occupancy of hydrogen failed.

The positions of these peaks attributed to hydrogen atoms within the β-PbO_2 cell are illustrated in Fig. 2. While only four of the eight symmetry equivalent H are illustrated, there would be four more equivalent positions in the second diagonal plane. We propose that for one Pb^{4+}, shown at the cell center in Fig. 2, four H atoms which are disordered are sited among the eight available sites. A more realistic picture is shown in Fig. 3, where the central Pb^{4+} is removed and four H are shown, two each in the two diagonal planes. To aid the reader, we show bonding to the two oxygen atoms nearest each H. These bond lengths correspond to one long bond near 2.5 Å and one short bond near 0.9 Å, lengths when

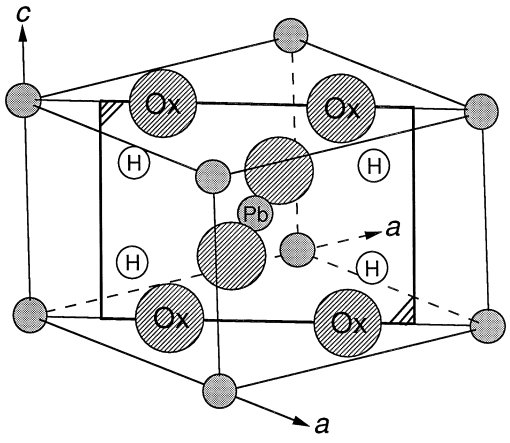

Fig. 2. Position of H within unit cell of β-PbO_2. Four of eight possible hydrogen positions are shown all of which lie on the illustrated diagonal plane. Four additional H positions would lie on a second diagonal plane perpendicular to the plane shown. The central Pb^{4+} also lies on the diagonal plane and is surrounded by six oxygen atoms.

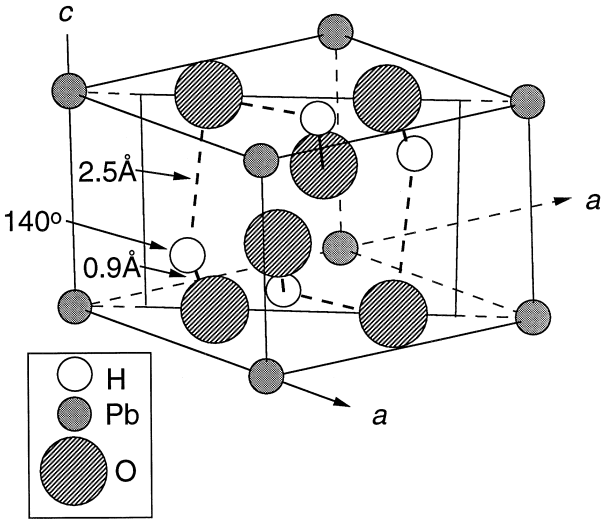

Fig. 3. Actual unit cell of β-PbO_2 in which the central Pb^{4+} has been removed and four H atoms are placed maintaining charge balance. Each of the four H atoms lie close to one oxygen forming an OH group but is also linked by a long bond to a second oxygen atom with a geometry typical of hydrogen bonding. Only four of the eight H sites are occupied leading to disordered hydrogen where various combinations of the eight sites can be occupied.

combined with the O−H···O bond angle of 140° are typical of hydrogen bonding.

This type of substitution is consistent with the deficiency of Pb relative to oxygen and the occurrence of H in β-PbO_2 structure. This proposed geometry based on diffraction data does not preclude the presence of Pb^{2+} or vacancies within β-PbO_2 as proposed by others, e.g. [3]. Combinations of vacancies (Pb^{2+}) surficial hydrogen in the form of OH or H_2O all add complications which makes the interpretation of bulk H, Pb, and O analyses difficult. Possibly various combinations lead to the difficulty in applying a single internally consistent chemical formula to explain observed chemical data [3]. We believe that our measurements are the first which show structural H in the β-PbO_2 structure.

2.4. Possible implications of hydrogen in β-PbO_2

The chemical formula of has been discussed and various representations put forth to explain the range of chemical determinations. Based on the above results, we propose the following: $Pb_{1-x}O_2H_{4x}$, where $0.92 < x < 0.97$. This representation can be modified to incorporate both Pb^{2+} and/or vacancies as required by other types of analyses, but these cannot be determined using diffraction data. Other evidence exists for the Pb ↔ 4H substitution in the β-PbO_2 lattice based mainly on neutron diffraction studies. In reference [6], 3–5% vacancy was deduced on the Pb site and using a deuterated sample, 0.21 H were present per PbO_2 unit. In reference [7], a deficiency of Pb relative to O was determined for four samples, where the lead fraction ranged from 0.95 to 0.99 in β-PbO_2. Evidence for O−H···O groups

within β-PbO_2 was reported in [8] supporting the geometry deduced from the present diffraction study.

While the non-stoichiometry of PbO_2 has been previously discussed, the description based on our neutron diffraction provides direct evidence for non-stoichiometry, the presence of a H crystallographic site, and disordered vacancies within that H site. The electrical conductivity of β-PbO_2 has been shown to be variable [12] and it has been proposed that this is related to non-stoichiometry, where free electron concentration increases as a result of H incorporation on interstitial sites [9]. From published results, the concentration of hydrogen decreases with cycling [10] and although our results cannot verify this for the samples studied, a reduction in hydrogen would tend to make the β-PbO_2 more stoichiometric, reduce related defects, and influence conductivity.

Many materials show different crystal morphologies and the specific cause of these morphology differences is not well known. Crystal growth rate, diffusion of components within the growth surroundings, and contamination of selective growth surfaces by trace or minor elements are all possibilities. From the above results, the major contaminant within β-PbO_2 is hydrogen. Recent quantitative measurements of the hydrogen content in the different crystallographic growth surfaces of natural quartz (SiO_2) shows that the development of specific growth forms is controlled in part by differences in the concentration of H-bearing species on specific growth faces [11]. By analogy, one might assume that H would have a similar effect of β-PbO_2 growth morphology. This is only a hypothesis, but the variation in PbO_2 growth morphology is well known to change from initial formation to failure (see later). The decrease in hydrogen content and change in growth morphology may result from the influence by hydrogen similar to that shown in quartz. However, confirmation would be especially difficult due to the extremely small crystallite size.

3. High resolution SEM imaging

Both the nine sample sequence of Cominco samples and the 12 sample sequence of laboratory cycled samples were imaged using a Hitachi S-4500 field emisson SEM. This instrument was operated at 3 kV and secondary electrons collected by extraction through the lens to obtain highest spatial resolution with routine magnification to 50,000×. Images were recorded both on film and digitally. The main objective was to document the changes in crystal size and shape as a function of cycle life and as a function of charging type. The images selected for presentation are considered typical based on surveys of many areas on each sample.

3.1. Initial crystal morphology

The initial formed sample (Fig. 4) and three additional samples to 40 rapid charged cycles (Fig. 5) of the laboratory series showed a rather uniform morphology for β-PbO_2

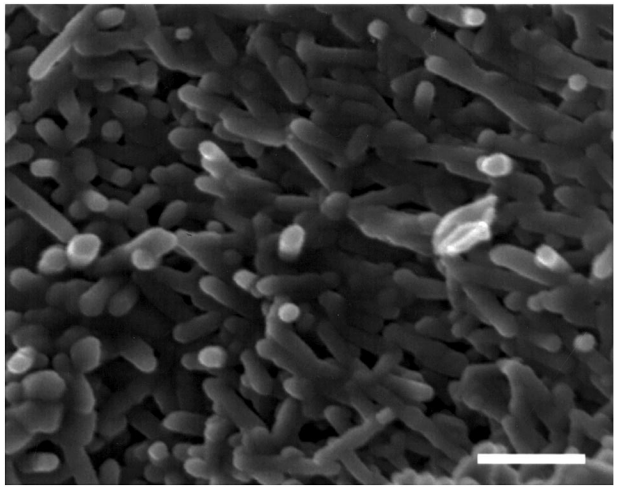

Fig. 4. Ten rapid charge cycles. β-PbO_2 shows a uniform grain size and shape with a typical length of ∼400 nm and a 10:1 aspect ratio. Scale bar = 400 nm in this and following images.

characterized by acicular grains (needle-shaped) with a length of approximately 400 nm and a length to width ratio of ∼10. Crystals usually grow in a sub-parallel orientation with some indication of crystallographic continuity among grains as seen by uniform orientation of crystal faces. This orientation suggests a relation between preexisting $PbSO_4$ and β-PbO_2, where one structure controls, to some extent, the orientation of the second during charging. This is best seen in Fig. 5, but is present in all samples showing a predominance of acicular grains. While the crystals are usually well formed, the last sample that shows apparent acicular crystals (Fig. 5) in fact has crystals where the faces are not flat, but rather show undulations along the length. This and the following images suggest that the crystal growth morphology is changing from a well-formed elongate crystal to a poorly formed elongate crystal to an equidimensional shape.

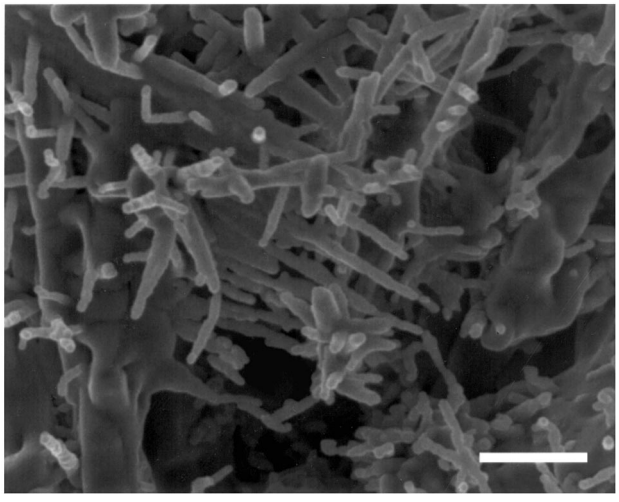

Fig. 5. Forty rapid charge cycles. β-PbO_2 crystals are not of uniform length and widths are variable within any one grain.

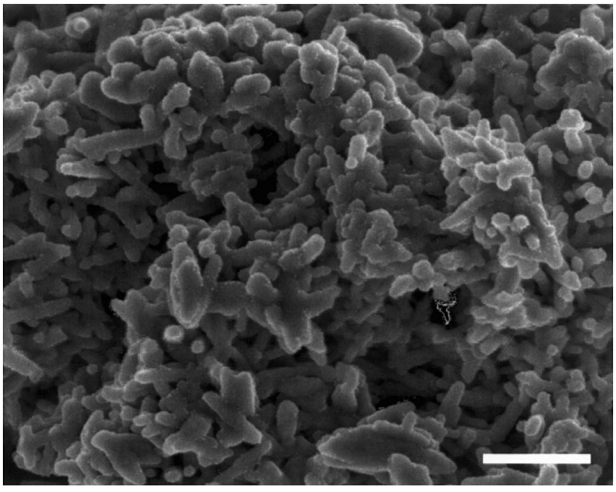

Fig. 6. Sixty rapid charge cycles. While some elongated grains are present, there is a distinct tendency toward small, equidimentional grains.

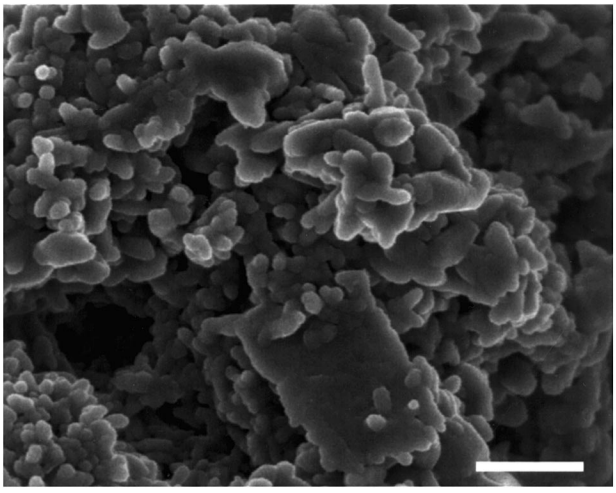

Fig. 8. Hundred rapid charge cycles. Small equidimentional grains of β-PbO_2 form large aggregates.

3.2. Intermediate and final morphology

Following cycle 40 for the laboratory cycled plates, elongate crystals are minor or absent. Figs. 6–9 show images of the active material at cycle at 60, 80, 100 and 120 cycles, respectively. While Fig. 6 does show some elongate crystals, they are essentially absent in the other three figures. Fig. 6 does show many equidimensional β-PbO_2 grains that have a ''diameter'' very similar to the width of the elongate grains in earlier cycles. The remaining figures show a progressively coarser grain size often with grains appearing to coalesce into micron-size units. Any characteristic morphology appears to be lost after approximately cycle 40.

3.3. Relation to morphology in Cominco active material

The characteristics of the morphology of the active β-PbO_2 in both the rapid and conventional charged active material from Cominco was previously described [3]. Briefly, the active positive material for both rapid and conventional charging series begins with acicular β-PbO_2 and progresses to an equidimentional and coarse material at failure. The evolution of the β-PbO_2 morphology appears to be the same and does not depend on the type of charging. In addition, the changes seen in the laboratory rapid charged sequence described here (Sections 3.1 and 3.2) are qualitatively identical to those observed in the Cominco material. Based on these sample sequences, we propose there is a evolution of β-PbO_2 morphology from initial formation to failure.

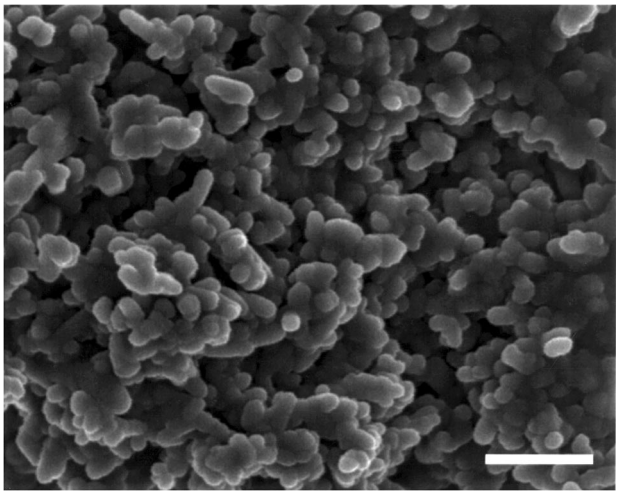

Fig. 9. One hundred and twenty rapid charge cycles. While many small equidimensional grains of β-PbO_2 can be seen, a coarse network of aggregates can be recognized.

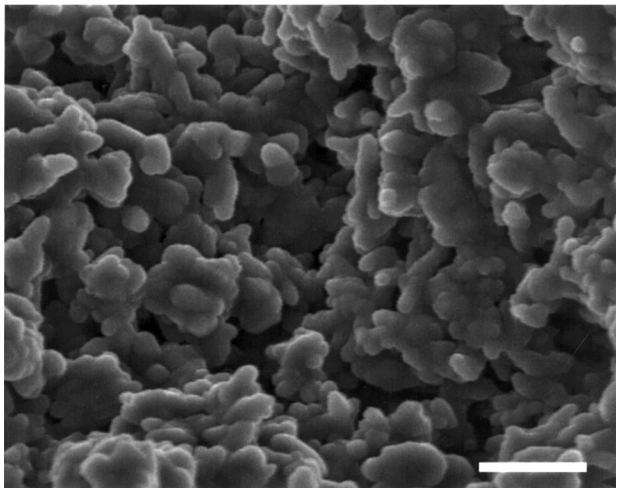

Fig. 7. Eight rapid charge cycles. Elongated β-PbO_2 crystals are rare or absent and individual grains have become larger than in Fig. 6.

4. Discussion

The association of H with β-PbO_2 is well known, but our determination of the location of H using neutron diffraction

provides direct evidence of its presence within the structure. The substitution is associated with Pb vacancies, close proximity to O to give an OH component, and hydrogen bonding characteristics. These observations support previous evidence based on nuclear magnetic resonance for the relation of H to the β-PbO_2 structure. The progressive change in β-PbO_2 stoichiometry from relatively Pb poor to more nearly stoichiometric β-PbO_2 confirms that the β-PbO_2 structure is Pb deficient and changes in a regular trend as β-PbO_2 forms and reforms during cycling. The disordered H and the Pb vacancies are defects which tend to decrease with cycling and should reduce the electrical conductivity of β-PbO_2 as cycling progresses. The observation of differences between chemical and electrochemical β-PbO_2 might well be related to the difference in H and hence defect levels. More subtle, and as yet unproven, effects of the changes in the H concentration of β-PbO_2 may be reflected in crystal morphology modification.

High magnification SEM images of positive active material that has undergone both rapid and conventional charging show a progressive change in grain morphology. It is not clear what is causing this change, but the progression from elongated, well-formed grains to equigranular crystals and finally to dense aggregates of grains results in a decrease in surface area for reaction with acid. The morphology changes appear to be similar for rapid and conventional charging and probably cannot explain the extended cycle life observed with rapid charging [1]. On the other hand, rapid charging may slow the progressive morphology change. While there is no a priori reason to relate the change in morphology with changes in the stoichiometry or hydrogen content of β-PbO_2, they both are at least crudely correlated. The extended cycle life observed with rapid charging may be related to the incorporation of H within the structure. Slow crystallization of β-PbO_2 during conventional charging may have the effect of excluding defects, in particular H, from the structure analogous to zone refining. Rapid charging, on the other hand, would promote rapid crystal growth and incorporation of defects. If defect concentration both promotes extended cycle life and is induced by rapid charging, charging regimes which incorporate both conventional and rapid charging may be beneficial. In particular, rapid charging may tend to increase defect concentration with associated H substitution.

Acknowledgements

This work was supported by the Advanced Lead Acid Battery Consortium (in Project no. β-004.1), a program of the International Lead Zinc Research Organization Inc. The generous sharing of material by Cominco Ltd. and GNB Technologies is appreciated. The Intense Pulsed Neutron Source at Argonne National Laboratory supported by the US Department of Energy, Basic Energy Sciences (DOE-BES) under Contract no. W-31-109-ENG-38.

References

[1] Cominco Inc., Final report for ALABC Projects RMC-002 and RMC-002A, 1997.
[2] I.M. Steele, J.J. Pluth, J.W. Richardson, in: IEEE 99TH8371. The Fourteenth Annual Battery Conference on Application and Advances, 1999, pp. 199–202. Proceedings of the Conference held at California State University, Long Beach, California.
[3] P. Ruetschi, R. Giovanoli, J. Power Sources 13 (1991) 81–97.
[4] P.T. Moseley, J.L. Hutchison, C.J. Wright, M.A.M. Bourke, R.J. Hill, V.S. Rainey, J. Electrochem. Soc. 130 (1983) 829–834.
[5] S.M. Caulder, A.C. Simon, J. Electrochem. Soc. 121 (1974) 1546–1551.
[6] J.D. Jorgensen, R. Varma, F.J. Rotella, G. Cook, N.P. Yao, J. Electrochem. Soc. 129 (1982) 1678–1681.
[7] R.J. Hill, Mater. Res. Bull. 17 (1982) 769–784.
[8] P. Boher, P. Garnier, J.R. Gavarri, J. Solid State Chem. 52 (1984) 146–155.
[9] J.P. Pohl, G.L. Schlechtriemen, J. Appl. Electrochem. 14 (1984) 521–531.
[10] S.M. Caulder, J.S. Murday, A.C. Simon, J. Electrochem. Soc. 120 (1973) 1515–1516.
[11] P.D. Ihinger, S.I. Zink, Nature 404 (2000) 865–868.
[12] E. Kress, J. Power Sources 4 (1979) 171–175.
[13] R.J. Hill, J. Power Sources 25 (1989) 313–320.